Hindawi
Concepts in Magnetic Resonance Part A, Bridging Education and Research
Volume 2023, Article ID 7007209, 8 pages
https://doi.org/10.1155/2023/7007209

Research Article

Analysis of Changes in Brain Region and Connectomics in the Acute Stage of Sudden Sensorineural Hearing Loss in the Resting State via Functional Magnetic Resonance Imaging

Zhonghua Li

Department of E.N.T.(Ear-Nose-Throat), Affiliated Hospital of Beihua University, Jilin City 132000, Jilin, China

Correspondence should be addressed to Zhonghua Li; 2020212235@mail.chzu.edu.cn

Received 30 July 2022; Revised 26 September 2022; Accepted 28 September 2022; Published 25 February 2023

Academic Editor: Enas Abdulhay

To explore the functional changes in the whole brain network in patients with sudden sensorineural hearing loss (SHL) at the acute stage from functional magnetic resonance imaging (fMRI) imaging evaluation results, 80 patients with sudden right SHL were selected as subjects (patient group). In addition, 40 healthy volunteers who underwent physical examination in the hospital during the same period were recruited as a control group. fMRI imaging was performed to analyze functional parameters and core nodes of the whole brain network. It was found that at all thresholds, the fMRI parameters C_p and L_p of the patient group were dramatically superior to those of the control group. The fMRI parameter E_{global} of the patient group was substantially lower than that of the control group ($P < 0.05$). At most of the thresholds, the fMRI parameter λ in patients was dramatically superior to that in the control group ($P < 0.05$). There were ten specific network core nodes in patients, including the right parahippocampal gyrus, right supra-occipital gyrus, left suboccipital gyrus, right fusiform gyrus, right parietal lobule, right subparietal lobule, right superior temporal gyrus, left superior marginal gyrus, and right superior temporal gyrus. In summary, the whole brains of patients with sudden SHL still had small-world attributes, but some characteristics of the brain network had changed, and there was a trend of transformation to a regular network. The connection between the auditory brain area and the functional areas related to language and vision was weakened, and the distribution of core nodes changed. This study provides a reference basis for exploring the changes in local brain and connectome levels in patients with sudden sensorineural hearing loss in the acute phase based on resting-state fMRI.

1. Introduction

When the lesions are in the hair cells, auditory nerves, or hearing centers at all levels of the helical organ and the sensation of sound and conduction of nerve impulses are impaired, resulting in hearing loss, it is called sensorineural hearing loss (SHL) [1–3]. Hearing loss caused by hair cell disease is called SHL (cochlear or terminal hearing loss). Hearing loss caused by lesions located in the auditory nerve and its conduction pathway is called neural hearing loss (retrocochlear or postcochlear) and is characterized by a marked decline in speech discrimination. Lesions occurring in the auditory center of the cerebral cortex are called central deafness and are often accompanied by neurological symptoms [4, 5]. SHL patients mainly have symptoms such as high-frequency hearing loss, reinvigorating phenomenon, tinnitus, and vertigo. This kind of deafness cannot change sound waves into nerve signals, or nerves, and their central way of producing obstacles cannot transmit nerve signals to the brain, which is the most difficult to treat and the most troublesome form of deafness. It is usually caused by congenital or acquired causes of cochlear auditory nerve or auditory center lesions, resulting in deafness [6–8]. According to current clinical and experimental studies, hearing loss often caused by SHL is irreversible and cannot be cured by drugs or surgery, which has been fully confirmed by massive basic and clinical studies and experiments over the years [9, 10]. Although the data showed that a small

number of people's sudden deafness can be cured automatically, for the occurrence of sudden deafness, it is still recommended for timely hospital diagnosis.

Common clinical diagnosis methods for deafness include vestibular function tests, hearing examinations, X-rays, computed tomography (CT), and MRI [11–14]. Patients with vertigo can undergo a cold temperature test and an electronystagmus examination to determine vestibular damage and exclude central dysfunction after the condition becomes stable [15]. Pure tone audiometry can show typical SHL, and the hearing curve of moderate, severe, or more severe hearing loss patients is usually flat or descending. The pure tone supramural function test, the Bekesy test, speech audiometry, and acoustic immittance test can determine cochlear deafness. X-ray or CT scans of the inner ear canal can rule out sudden deafness caused by external neuroma or other intracranial occupying lesions [16]. However, the above methods can only make a preliminary judgment on the lesion degree of patients but cannot evaluate the changes in cerebral cortical functional activities after deafness [17]. Functional magnetic resonance imaging (fMRI) is a new neuroimaging method that uses magnetic resonance imaging to measure the hemodynamic changes caused by neuronal activity. It has been widely used to map brain activation in humans and animals. The change of local deoxyhemoglobin concentration in the brain will lead to the change of magnetic resonance signal intensity, which indirectly reflects neuronal activity and then reflects the change of brain function in real time [18]. In recent years, fMRI has become the tool of choice for visualizing neural activity in the human brain due to its noninvasive nature, reproducibility, and lack of radiation exposure. In resting-state fMRI, subjects are scanned while lying flat, eyes closed, awake, and not thinking about a problem without a specific task. Resting-state fMRI is very suitable for the study of clinical diseases, especially neurological diseases because of its simple experimental design, simple operation, and ability to observe the spontaneous brain activity of subjects without subjects completing specific tasks [19]. The brain is one of the major parts of the central nervous system. It can transmit, store, and process information, make people do various psychological activities, and dominate and control people's behavior. Although they are composed of various brain regions that are independent of each other in space, these brain regions are functionally interconnected and constantly flow information with each other [20]. Therefore, it is significant to explore sudden deafness from the perspective of brain functional network changes.

In summary, this study aimed to analyze the functional parameters and core nodes of the whole brain network based on resting-state fMRI by conducting fMRI scanning and constructing the brain functional networks of 80 patients with severe right sensorineural hearing loss and 40 healthy volunteers. It was hoped to provide a reference for the study of the changes in the functional connectivity level of the whole brain network in patients with sudden sensorineural hearing loss in the acute stage.

2. Materials and Methods

2.1. Research Objects. Eighty patients with severe right SHL who visited the hospital from October 2019 to October 2021 were selected as study subjects (patient group), including 34 males and 46 females. The average age was 35.36 ± 10.34 years (range, 25–67 years). After pure tone audiometry, the hearing threshold of the affected ear of the patient group was more than 70 dB, and the hearing threshold of the healthy ear was in the normal range. In addition, 40 healthy volunteers who underwent physical examination in the hospital during the same period were selected as a control group, including 15 males and 25 females. The age ranged from 24 to 65 years, with an average age of 37.11 ± 8.95 years. After pure-tone audiometry, the hearing threshold of both ears was less than 25 dB. This study was approved by the ethics committee of the hospital. The subjects and their families were informed of the study and signed informed consent forms.

Inclusion criteria are as follows: (i) all subjects were right-handed; (ii) subjects had complete basic information; (iii) subjects had no previous history of mental illness; and (iv) subjects were older than 18 years.

Exclusion criteria are as follows: (i) subjects with contraindications to MRI examination; (ii) subjects with history of cardiovascular disease; and (iii) subjects complicated with serious damage to the heart, liver, and kidney organs.

2.2. Resting fMRI Examination. A 3.0 T superconducting magnetic resonance imaging system with 12 channel coils was used. First, the subjects were placed in a supine position and put on an eye mask and soundproof earplugs to avoid interference from the outside environment. The subjects were guided to remain in a resting state. After the scan, if the patient was found not to remain in a resting state during the scan, the sample would be removed. A total of 300 time points were collected by resting whole brain volume scanning for each subject. The scanning parameters were as follows: repeat time (TR) = 1.800 ms, echo time (TE) = 20 ms, layer thickness = 3.5 ms, layer spacing = 0, layer number = 65, field of vision = 256 × 256, matrix = 256 × 256, and flip angle = 90 degrees.

2.3. Image Preprocessing. The data processing assistant for resting-state fMRI (DPARSF) based on MATLAB R2014b-2020b was used to preprocess the obtained images. The volume data of the first 10 points of each subject were removed. Time correction and head correction were carried out for the remaining 290 time points. Sample data of head movement exceeding 2 mm and rotation exceeding 2 degrees were removed. Linear regression was adopted to remove white matter and cerebrospinal fluid signals from the image data, and then it was standardized to the spatial coordinates of the Montreal Neurological Institute for resampling. Spatial smoothing was performed on standardized data, and time-domain bandpass filtering with a bandwidth of approximately 0.05 Hz was used to reduce the

influence of low-frequency drift and high-frequency physiological noise.

2.4. Construction of the Brain Functional Network. GRETNA, developed by Professor Yong He's team from Beijing Normal University, was used to construct the brain functional networks of subjects. The subjects' brains were registered on an automatic anatomical marker map, which divided the cerebral cortex into 90 regions. Each region represented a node, and the time correlation of the blood oxygen level-dependent signal in each brain region was called an edge. The average time series of all voxels in each brain region was extracted, and the Pearson correlation coefficient between them was calculated to obtain the correlation matrix R. Then, the Fisher Z transformation was performed on the matrix R to obtain the correlation matrix Z, which was converted to the correlation matrix C for parameter calculation.

2.5. Brain Functional Network Parameters. Given that the network node set is U and the network edge set is I, the complex network can be represented by the image $F(U\ and\ I)$. Then, the node clustering coefficient C_x is expressed as follows:

$$C_x = \frac{2E_x}{L_x(L_x-1)} C_y = \frac{2E_y}{L_y(L_y-1)}. \quad (1)$$

L_x represents the number of nodes constituting subgraph F_x, L_y represents the number of nodes constituting subgraph F_y, and E represents local efficiency. The average value of C_x of all nodes is the network clustering coefficient C_p, which can be used to evaluate the degree of network collectivization. The average value of E_x of all nodes is the network local efficiency E_{local}, which can be used to evaluate the network defense capability. The average maximum short-circuit length L_p is the average time l_{xy} of all nodes to ensure effective integration and fast transmission of information in distant brain regions. Global efficiency E_{global} evaluates the global transport capacity of a network.

The standardized coefficient γ reflects the transformation from the real brain network to the regular network, and the standardized average shortest path length λ reflects the transformation from the real brain network to the random network, which can be expressed as follows:

$$\gamma = \frac{C_p}{C_{\text{rand}}},$$
$$\lambda = \frac{L_p}{L_{\text{rand}}}, \quad (2)$$
$$\sigma = \frac{\gamma}{\lambda}.$$

C_{rand} represents the clustering coefficient of the random network, L_{rand} represents the shortest path length of the random network, and $\sigma > 1$ indicates that the network has a high clustering coefficient and a short characteristic path length.

The intermediate centricity method was used to find the core nodes of the whole brain network. In this experiment, the threshold range was 0.1–0.2 with an interval of 0.02.

2.6. Statistical Methods. SPSS 19.0 statistical software was used for data processing in this study. The mean ± standard deviation ($\overline{x} \pm s$) was used for measurement data, and the percentage (%) was used for counting data. Pairwise comparison was performed by one-way ANOVA. $P < 0.05$ suggests that the difference was statistically significant.

3. Results

3.1. General Information. In Table 1, the ratio of male to female, age, course of disease, height, weight, years of education, THI score, and left ear PTA score in the patient group were not significantly different from those in the normal group ($P > 0.05$). The PTA score of the patient group (85.71 ± 9.01) was significantly higher than that of the normal group (20.77 ± 3.81), and the difference was statistically significant ($P < 0.05$).

3.2. Comparison of fMRI Global Parameters. Figure 1 shows the comparison of the fMRI parameters E_{global}, E_{local}, C_p, and L_p between the two groups. The fMRI parameters E_{global}, E_{local}, and C_p of the two groups showed an increasing trend with an increasing threshold, while L_p showed a decreasing trend with an increasing threshold. At all thresholds, the fMRI parameters, C_p and L_p, in patients were dramatically superior to those in the control group, and the differences were considerable ($P < 0.05$). At most of the thresholds, the fMRI parameter E_{global} of the patient group was substantially lower than that of the control group, and the differences were considerable ($P < 0.05$). At all thresholds, there was no considerable difference in the fMRI parameter E_{local} between the patient group and the control group ($P > 0.05$).

Figure 2 shows the comparison of fMRI parameters γ, λ, and σ between the two groups. The fMRI parameters γ, λ and σ of the two groups showed a decreasing trend with an increasing threshold value. At most of the thresholds, the fMRI parameter λ of the patient group was dramatically superior to that of the control group, and the differences were considerable ($P < 0.05$). At all thresholds, fMRI parameters γ and σ in the patient group were not substantially different from those in the control group ($P > 0.05$).

3.3. FMRI Image Data. Figure 3 shows MRI images of one patient in the patient group. Physical examination suggested a clear mind, vague language, decreased vision, no nystagmus, deafness in both ears, muscle strength level V, bilateral calcaneus shin test (+), and acceptable finger and nose rotation. Obviously, the surface of the midbrain, pons, vermis of the cerebellum and sulci, bilateral lateral fissure, underside of the frontal lobe, and spinal cord were surrounded by short T2 signals with bands.

Table 1: Comparison of basic data of medical staff between the two groups.

Basic information	Patient group ($n = 80$)	Control group ($n = 40$)	P
Sex ratio (male/female)	42.5/57.5	37.5/62.5	1.457
Age (years old)	35.36 ± 10.34	37.11 ± 8.95	2.568
Duration of disease (days)	9.16 ± 1.76	—	—
Height (cm)	160.44 ± 11.42	158.33 ± 10.68	1.496
Body weight (kg)	57.03 ± 5.82	55.81 ± 7.03	1.733
Years of education (years)	12.35 ± 3.25	11.09 ± 2.88	2.024
THI score (points)	49.68 ± 13.06	51.66 ± 16.77	2.145
Auris sinistra/Auris dextra	$21.74 \pm 4.11/85.71 \pm 9.01$	$21.33 \pm 3.57/20.77 \pm 3.81^*$	0.0378

*indicated a statistically significant difference compared with the patient group ($P < 0.05$).

Figure 4 shows the MRI data of a healthy volunteer in the control group. The T1 weighted image presented a high signal, and the T2 weighted image presented an equal signal. The position of the brain stem and cerebellum was normal without displacement or deformation, and the surface of the midbrain, pons, vermis, and sulci was normal.

3.4. Analysis Results of Functional Core Nodes of the Whole Brain Network. In Figure 5, this analysis showed that there were 10 specific network core nodes in the patient group, including the right parahippocampal gyrus, right suproccipital gyrus, left suproccipital gyrus, right fusiform gyrus, right parietal lobule, right subparietal lobule, right superior temporal gyrus, left superior marginal gyrus, and right superior temporal gyrus temporal pole. There were eight specific network core nodes in the control group, including the left inferior frontal gyrus orbital, right insula, left insula, left parietal lobule,, right pea shell, left superior temporal gyrus temporal pole, and right middle temporal gyrus temporal pole. Subjects in both groups had a total of five network core nodes, including the right inferior frontal gyrus orbital region, left posterior central gyrus, right superior marginal gyrus, left middle cingulate gyrus, and right superior frontal gyrus medial orbital region.

4. Discussion

Sudden sensorineural deafness refers to the sudden occurrence of SHL of unknown cause, which can develop from mild hearing loss to severe hearing loss within minutes, hours, or 1–2 days [21]. There is no specific diagnosis and treatment method for approximately 90% of cases of sudden sensorineural deafness because the cause is unclear. In addition, the lack of high-quality clinical research and evidence-based medical proof makes the diagnosis and treatment of sudden inductive neural deafness controversial. Therefore, seeking an efficient diagnostic method is a reliable way to achieve clinical treatment optimization [22]. In this study, 80 patients with severe right SHL who visited the hospital were selected as the study subjects (patient group), and 40 healthy volunteers who underwent physical examination in the hospital during the same period were selected as the control group. FMRI imaging was performed on all patients. GRETNA was used to construct the subjects' brain functional networks, and the functional parameters and core nodes of the whole brain network were analyzed. First, the basic data of the two groups of subjects were compared. The results showed that the ratio of males to females, age, course of disease, height, weight, years of education, THI score, and left ear PTA score in the patient group were not significantly different from those in the control group ($P > 0.05$), which provided a baseline for subsequent studies. In addition, the PTA score of the patient group (85.71 ± 9.01) was dramatically superior to that of the control group (20.77 ± 3.81), and the difference was significant ($P < 0.05$), which was consistent with the control study between the patient group and control group.

The functional network of the human brain is a complex and real network between a random network and a regular network, and its small-world attributes can ensure that the brain can efficiently integrate and separate information under relatively low energy consumption [23]. This study found that at all thresholds, the fMRI parameters C_p and L_p of the patient group were dramatically superior to those of the control group. At most of the thresholds, the fMRI parameter E_{global} of the patient group was substantially lower than that of the control group, and the differences were considerable ($P < 0.05$). This is generally consistent with the research results of Minosse et al. [24]. Although the whole brain of patients with sudden sensorineural hearing loss still had the small-world property, some characteristics of the brain network had changed. The increase of parameters meant that the information processing ability of some brain regions of patients was enhanced, indicating that the contralateral superiority of hearing conduction was weakened, and intrachannel reorganization occurred in the auditory cortex. The increase in parameters L_p and E_{local} suggested that the information processing ability of the patient's remote brain region was weakened, which was consistent with the general deletion hypothesis [25]. At most of the thresholds, the fMRI parameter λ of the patient group was dramatically superior to that of the control group, and the differences were considerable ($P < 0.05$). At all thresholds, fMRI parameters γ and σ in the patient group were not substantially different from those in the control group ($P > 0.05$). Wang et al. [26] also pointed out that this indicates that the brain functional network of patients with sudden sensorineural hearing loss has a trend of changing to a regular network, with enhanced information integration ability and weakened separation transmission ability. The results indicate that the brain functional network of patients

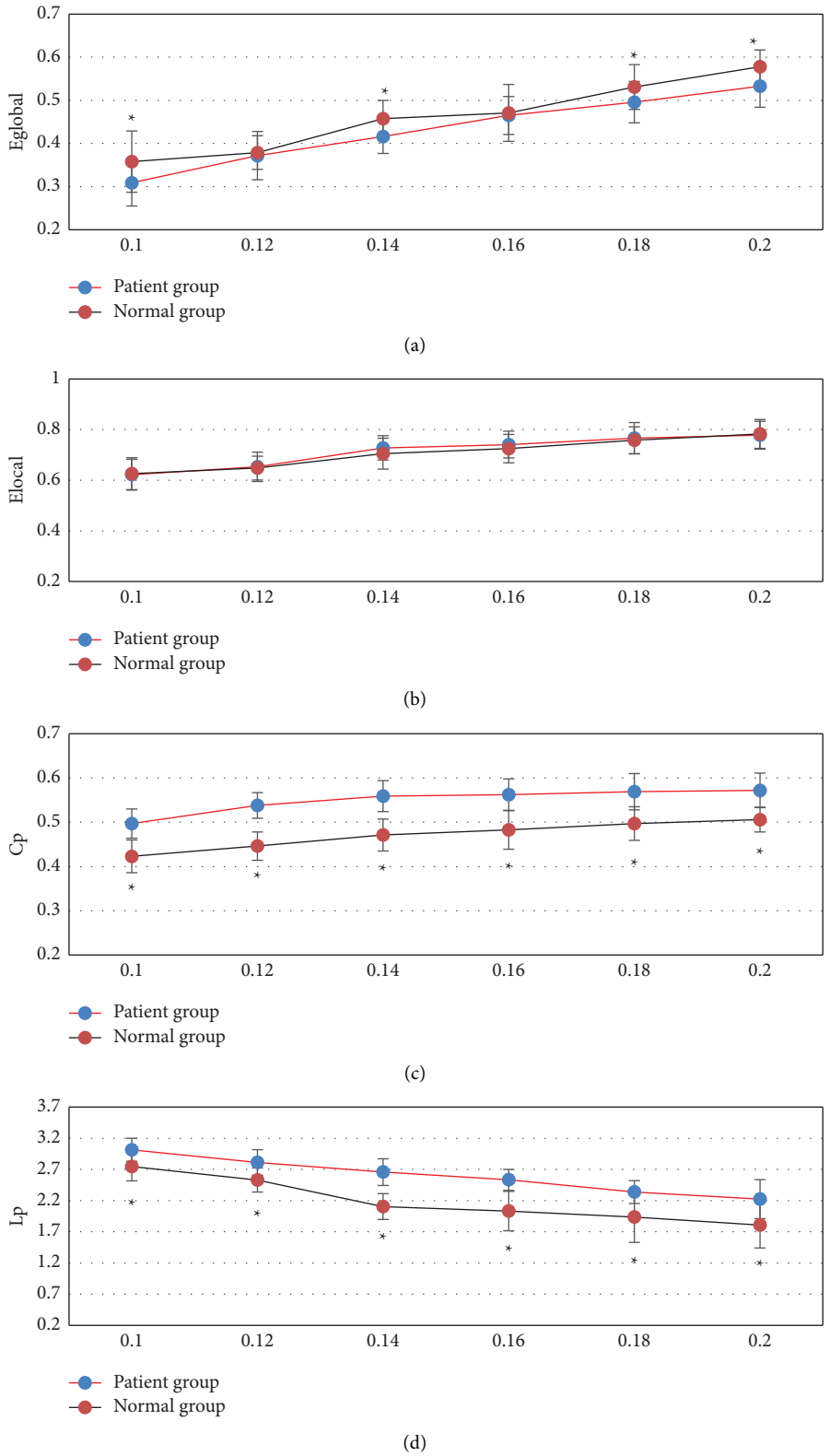

FIGURE 1: Comparison of the fMRI parameters E_{global}, E_{local}, C_p, and L_p between the two groups. (a–d) represented E_{global}, E_{local}, C_p, and L_p, respectively. *represents that the fMRI parameters of the patient group, including E_{global}, C_p, and L_p, were significantly different from those in the normal group ($P < 0.05$).

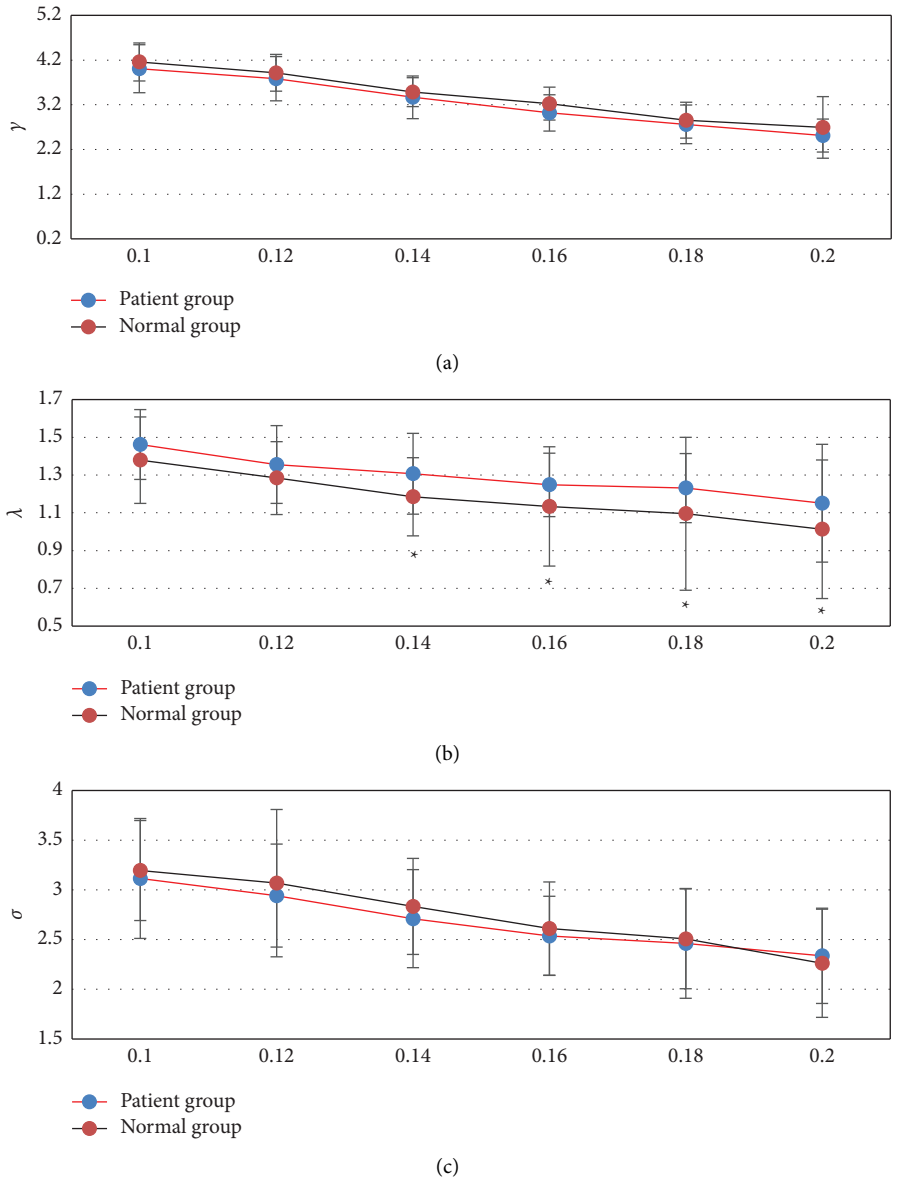

Figure 2: Comparison of fMRI parameters γ, λ, and σ between the two groups. (a–c) represented γ, λ, and σ, respectively. *Compared with the normal group, $P < 0.05$.

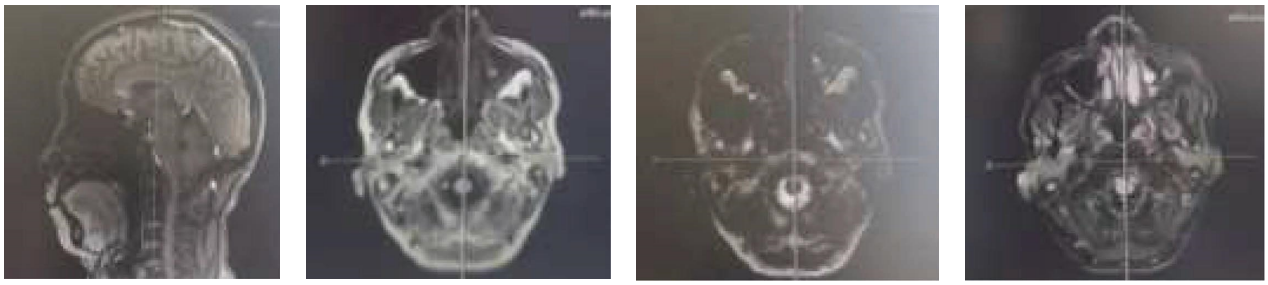

Figure 3: MRI image data of a patient. Female, 58 years old, high tinnitus in both ears without obvious inducement, followed by hearing loss, and gradually aggravated, with basic hearing loss in the recent six months, unstable walking, and tremor on both upper limbs. (a) MRI sagittal image; (b-c) T1 weighted image; and (d) T2 weighted image.

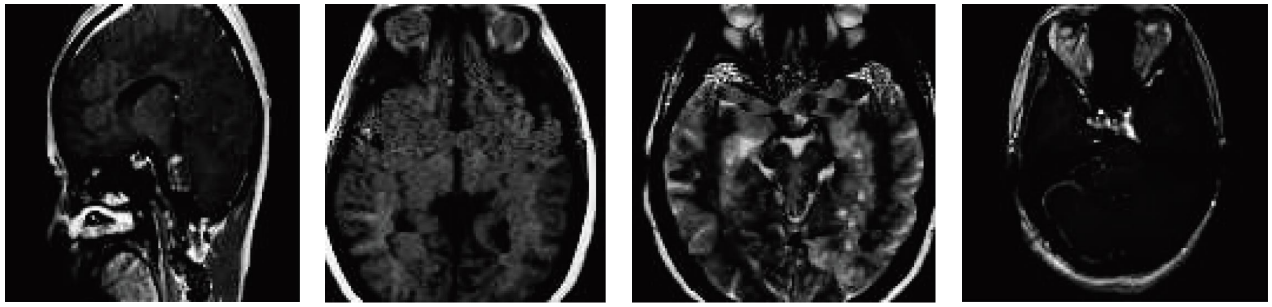

Figure 4: MRI image data of a healthy volunteer in the control group. Female, 50 years old, physical examination showed normal body function but no liver or kidney damage. (a) MRI sagittal image; (b-c) T1 weighted image; (d) T2 weighted image.

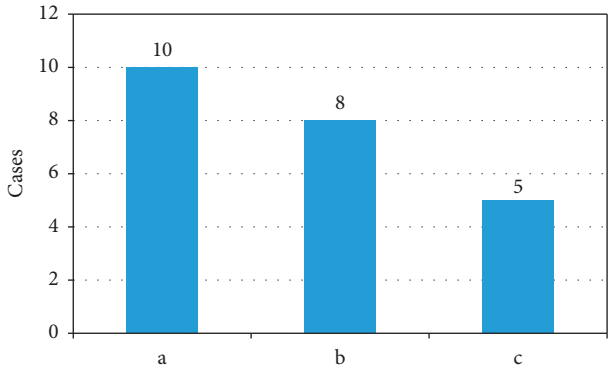

Figure 5: Analysis results of functional core nodes of the whole brain network in two groups. (a) The specific network core node of patient group; (b) the network core node unique to control group; and (c) the network core nodes shared by both groups.

with sudden SHL tended to change to a regular network, and the ability of information integration was enhanced, while the ability of separation and transmission was weakened. All the above results confirm to some extent that the connection between auditory brain areas and language and vision-related functional areas was weakened in patients with burst SHL, and their language perception and understanding ability were decreased [27].

There were ten specific network core nodes in patients, including the right parahippocampal gyrus, right supraoccipital gyrus, left suboccipital gyrus, right fusiform gyrus, right parietal lobule, right subparietal lobule, right superior temporal gyrus, and left superior marginal gyrus. Among them, the superior occipital gyrus, fusiform gyrus, superior marginal gyrus, temporal pole, inferior parietal lobule, and parietal lobule are related to visual and auditory information processing. The increase in the importance of these core nodes indicates that other sensory channels are compensatory and that the advantage of coping is weakened after hearing loss. There were eight specific network core nodes in the control group, including the left inferior frontal gyrus orbital, right insula, left insula, left parietal lobule, left parietal lobule, right pea shell, left superior temporal gyrus temporal pole, and right middle temporal gyrus temporal pole. Most of these nodes belong to the limbic or parlimbic system, but they were absent in the patient group, possibly because of the recombination of these nodes after deafness [28].

5. Conclusion

In this study, the functional parameters and core nodes of the whole brain network were analyzed by fMRI scanning and GRETNA software to construct the brain functional network of subjects. The results showed that the brains of patients with sudden sensorineural deafness still had a small-world nature. However, some characteristics of the brain network had changed, and there was a trend to transform to a regular network. The connection between the auditory brain region and language and visual related functional regions was weakened, and the distribution of core nodes was changed, which enhanced the information integration ability of local brain regions and weakened the separation transmission ability. However, the limitation of this study is that the included sample size was small and all of them were from the same hospital, and the evaluation of patient samples was insufficient. The visual and language function evaluation data of the patients were not obtained from the side, and the correlation between right deafness and different functions could not be verified. Therefore, the sample size will be expanded in the later stage, and the patient case data will be increased to explore the difference in brain network function between left and right deafness patients. In conclusion, this study provides data reference for the study of brain network function in patients with sudden right sensorineural hearing loss.

Data Availability

The data used to support the findings of this study are available from the corresponding author upon request.

Conflicts of Interest

The author declares that there are no conflicts of interest.

References

[1] M. Herrera, J. R. García Berrocal, A. García Arumí, M. J. Lavilla, G. Plaza, and Grupo de Trabajo de la Comisión de Audiología de la SEORL, "Update on consensus on diagnosis and treatment of idiopathic sudden sensorineural hearing loss," *Acta Otorrinolaringológica Española*, vol. 70, no. 5, pp. 290–300, 2019.

[2] J. Jeong and H. S. Choi, "Sudden sensorineural hearing loss after COVID-19 vaccination," *International Journal of Infectious Diseases*, vol. 113, pp. 341–343, 2021.

[3] Y. H. Young, "Contemporary review of the causes and differential diagnosis of sudden sensorineural hearing loss," *International Journal of Audiology*, vol. 59, no. 4, pp. 243–253, 2020.

[4] J. G. Doo, D. Kim, Y. Kim et al., "Biomarkers suggesting favorable prognostic outcomes in sudden sensorineural hearing loss," *International Journal of Molecular Sciences*, vol. 21, no. 19, p. 7248, 2020.

[5] M. Marx, E. Younes, S. S. Chandrasekhar et al., "International consensus (ICON) on treatment of sudden sensorineural hearing loss," *European Annals of Otorhinolaryngology, Head and Neck Diseases*, vol. 135, no. 1, pp. S23–S28, 2018.

[6] J. W. Wood, A. D. Shaffer, D. Kitsko, and D. H. Chi, "Sudden sensorineural hearing loss in children-management and outcomes: a meta-analysis," *The Laryngoscope*, vol. 131, no. 2, pp. 425–434, 2021.

[7] Y. C. Chen, S. J. Tsai, J. C. Chen, and J. H. Hwang, "Risks of tinnitus, sensorineural hearing impairment, and sudden deafness in patients with non-migraine headache," *PLoS One*, vol. 14, no. 9, Article ID e0222041, 2019.

[8] C. Mirian and T. Ovesen, "Intratympanic vs. systemic corticosteroids in first-line treatment of idiopathic sudden sensorineural hearing loss: a systematic review and meta-analysis," *JAMA Otolaryngol Head Neck Surg*, vol. 146, no. 5, pp. 421–428, 2020.

[9] T. M. Rhee, D. Hwang, J. S. Lee, J. Park, and J. M. Lee, "Addition of hyperbaric oxygen therapy vs. medical therapy alone for idiopathic sudden sensorineural hearing loss: a systematic review and meta-analysis," *JAMA Otolaryngol Head Neck Surg*, vol. 144, no. 12, pp. 1153–1161, 2018.

[10] A. Ponzetto, G. Cavallo, and N. Figura, "Sudden sensorineural hearing loss," *JAMA Otolaryngol Head Neck Surg*, vol. 146, no. 2, p. 211, 2020.

[11] A. D. P. Prince and E. Z. Stucken, "Sudden sensorineural hearing loss: a diagnostic and therapeutic emergency," *The Journal of the American Board of Family Medicine*, vol. 34, no. 1, pp. 216–223, 2021.

[12] J. W. Ma and J. C. C. Wei, "Correspondence on: "Antidepressants and risk of sudden sensorineural hearing loss"," *International Journal of Epidemiology*, vol. 50, no. 5, pp. 1748-1749, 2021.

[13] H. Zhang, W. Lv, H. Diao, and L. Shang, "Reconstruction algorithm-based CT imaging for the diagnosis of hepatic ascites," *Computational and Mathematical Methods in Medicine*, vol. 2022, Article ID 1809186, 11 pages, 2022.

[14] M. M. Wang, Y. J. Wang, N. Hu et al., "3D-FLAIR MRI findings in idiopathic sudden sensorineural hearing loss and the correlations with clinical features and prognosis," *Zhonghua er bi Yan Hou Tou Jing Wai ke za Zhi*, vol. 56, no. 5, pp. 424–430, 2021.

[15] J. Wang, T. Ren, W. Sun, Q. Liang, and W. Wang, "Post-contrast 3D-FLAIR in idiopathic sudden sensorineural hearing loss," *European Archives of Oto-Rhino-Laryngology*, vol. 276, no. 5, pp. 1291–1299, 2019.

[16] Y. Islamoglu, G. G. Kesici, K. Ercan, and M. A. Bababemez, "Single-sided deafness after sudden hearıng loss: late effect on cochlear nerve size," *European Archives of Oto-Rhino-Laryngology*, vol. 277, no. 9, pp. 2423–2426, 2020.

[17] X. Min, H. Gu, Y. Zhang, K. Li, Z. Pan, and T. Jiang, "Clinical value of abnormal MRI findings in patients with unilateral sudden sensorineural hearing loss," *Diagn Interv Radiol*, vol. 26, no. 5, pp. 429–436, 2020.

[18] C. J. Yang, T. Yoshida, S. Sugimoto et al., "Lesion-specific prognosis by magnetic resonance imaging in sudden sensorineural hearing loss," *Acta Oto-Laryngologica*, vol. 141, no. 1, pp. 5–9, 2021.

[19] X. Chen, Q. Zhang, C. Yang, Y. Liu, and L. Li, "GRβ regulates glucocorticoid resistance in sudden sensorineural hearing loss," *Current Pharmaceutical Biotechnology*, vol. 22, no. 9, pp. 1206–1215, 2021.

[20] N. Mehta and S. Mehta, "Comparative evaluation of injection dexamethasone and oral glycerol versus injection dexamethasone alone in the treatment of sudden onset sensorineural deafness," *Ear, Nose, & Throat Journal*, vol. 100, pp. 317S–324S, 2021.

[21] T. G. Joshua, A. Ayub, P. Wijesinghe, and D. A. Nunez, "Hyperbaric oxygen therapy for patients with sudden sensorineural hearing loss: a systematic review and meta-analysis," *JAMA Otolaryngol Head Neck Surg*, vol. 148, no. 1, pp. 5–11, 2022.

[22] W. W. Jung and C. Hoegerl, "Sudden sensorineural hearing loss and why it's an emergency," *Cureus*, vol. 14, no. 1, Article ID e21418, 2022.

[23] H. Wong, Y. Amoako-Tuffour, K. Faiz, and J. J. S. Shankar, "Diagnostic yield of MRI for sensorineural hearing loss - an audit," *The Canadian Journal of Neurological Sciences*, vol. 47, no. 5, pp. 656–660, 2020.

[24] S. Minosse, F. Garaci, F. Martino et al., "Global and local brain connectivity changes associated with sudden unilateral sensorineural hearing loss," *NMR in Biomedicine*, vol. 34, no. 8, Article ID e4544, 2021.

[25] R. G. Yoon, Y. Choi, and H. J. Park, "Clinical usefulness of labyrinthine three-dimensional fluid-attenuated inversion recovery magnetic resonance images in idiopathic sudden sensorineural hearing loss," *Current Opinion in Otolaryngology & Head and Neck Surgery*, vol. 29, no. 5, pp. 349–356, 2021.

[26] S. Wang, B. Chen, Y. Yu et al., "Altered resting-state functional network connectivity in profound sensorineural hearing loss infants within an early sensitive period: a group ICA study," *Human Brain Mapping*, vol. 42, no. 13, pp. 4314–4326, 2021.

[27] M. Wang, N. Hu, Y. Wang, X. Sun, Z. Fan, and H. Wang, "Clinical value of 3D-FLAIR MRI in idiopathic sudden sensorineural hearing loss," *ACS Chemical Neuroscience*, vol. 13, no. 1, pp. 151–157, 2022.

[28] L. D. Dumberger, T. P. Hwa, K. Panara, S. Husain, C. Yver, and D. C. Bigelow, "Profound sudden sensorineural hearing loss in hematologic malignancy: a case for urgent cochlear implantation with discussion and systematic review of the literature," *Otology & Neurotology*, vol. 42, no. 7, pp. e815–e824, 2021.